Numerical simulation for flow field inside pintle thruster for solid attitude orbit control system

XUE Bin[1], CHENG Cheng[2], WANG Yibai[1], CHANG Heng[1], LIU Yu[1]
(1. School of Astronautics, Beihang University, Beijing 100191, China;
2. Shanghai Institute of Space Propulsion, Shanghai 201112, China)

Abstract: In order to investigate the characteristics and roles of flow field inside pintle thruster, a two-dimensional axisymmetric model is used to carry out unsteady and steady state flow field simulation during the pintle moving process. The flow field structures, aerodynamic force and flow field sensitivity to geometrical parameter of the pintle at different opening are analyzed. The analysis result shows that the phenomena of complex shockwave and tip separation occur in the flow field structure because of the pintle's disturbance, the aerodynamic coefficient increases with the increase of cone angle section area of pintle tip, but seems to have no obvious relationship with pressure intensity of the chamber. The results also show that the throttling surface shape can strongly influence the flow pattern such as flow parameter distribution, shockwave strength and location, and aerodynamic force.

Keywords: solid attitude orbit control system; pintle thruster; unsteady flow field; dynamic mesh
CLC Number: V435.1-34 **Document code**: A **Article ID**: 1672-9374 (2016) 06-0020-05

固体姿轨控针栓推力器内流场数值仿真

薛 斌[1], 程 诚[2], 王一白[1], 常 桁[1], 刘 宇[1]
(1. 北京航空航天大学宇航学院, 北京 100191; 2. 上海空间推进研究所; 上海 201112)

摘 要: 为研究针栓推力器内流场的特征和规律, 采用二维轴对称模型, 开展了针栓运动过程的非稳态及稳态流场仿真, 分析了不同开度下的流场结构、针栓所受气动力及流场对针栓几何参数的敏感性。结果表明: 由于针栓的干扰作用, 流场结构呈现出复杂激波系、顶端流动分离等现象; 气动力系数与针栓头部锥角大小呈正相关关系, 与集气室压强无关; 节流面形状对气流参数分布、激波强度及位置、气动力等表征的流动模态影响很大。

关键词: 固体姿轨控系统; 针栓推力器; 非稳态流场; 动网格
中图分类号: V435.1-34 **文献标识码**: A **文章编号**: 1672-9374 (2016) 06-0020-05

Received date: 2016-02-25; Revised date: 2016-05-13
Biography: XUE Bin (1991—) , male, graduate student for a Master's degree, speciality: research on solid rocket engines

0 Introduction

Solid rocket motors (SRM) have been widely used in many platforms including sounding rockets, tactical missiles and launch vehicle boosters because of their inherent advantages: simplicity, easy storage, light weight and low cost. Thrust throttling technology has been developed to deal with the problem, giving SRM the ability to adjust thrust[1-2]. By adjusting the position of a pintle assigned axially with the nozzle, throat area is changed and thrust is variable[3]. To make full use of the advantages, thrust throttling technology is applied in solid divert and attitude control system (SDACS) by integrating multiple pintle thrusters with a solid gas generator[4-5]. Different with the single pintle motor, chamber pressure and variable mass flow rate in SDACS are maintained at a given constant value through differential co-work mode of every two thrusters[6].

To find breakthrough technologies and realize good performance of SDACS with high chamber pressure, numerous research on pintle thrusters have been done during the past years. Integral thruster of ceramic matrix composite material were designed and manufactured, and then tested by hover tests and cold flow experiments[7-9]. To establish the characteristics of the propulsive efficiency and the aerodynamic load on the pintle, Lafond investigated the inside flowfield in steady state of divert nozzle numerically[10]. In addition, the control loop and algorithm of SDACS were studied by Aussignac and Jouner[11-12].

Nevertheless, there are few unsteady numerical research about inside flowfield of pintle thruster, which are important to a certain degree because the pintle motion is a dynamic process. In the present study, inside flowfield in a pintle thruster of SDACS is studied through CFD method with dynamic mesh. The pintle motion velocity is given from previous study. Typical flow pattern of pintle thruster is analyzed, including complex shock waves and subsonic circumfluence zone at the pintle tip. A dimensionless coefficient is defined to investigate the law of the aerodynamic force. Then influences of thruster opening on flowfield and aerodynamic force are analyzed. What's more, based on steady state of 1.0 opening, several cases with variable key parameters are calculated to study the geometrical sensitivity of inside flowfield.

1 Numerical modeling

1.1 Computational grid and boundary conditions

The schematic diagram of the SDACS thruster is presented in Fig. 1. The thruster is a kind of on-off valve with a Needle-shaped pintle concentric with the throat. That is, the thruster can only be in the "open" position or in the "close" position. The pintle motion is controlled by a solenoid, which receives the pulse width modulation (PWM) signal to switch on-off state of the thruster. The averaged thrust produced by the nozzle is proportional with the duty ratio in working cycles.

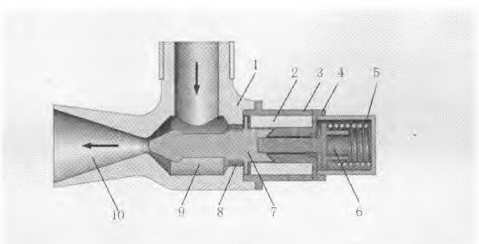

1–Valve seat; 2–Coil; 3–Shell; 4–Middle plate; 5–Spring shell; 6–Push rod;. 7–Pintle; 8–Magnetism isolating ring; 9–Nozzle chamber; 10–Nozzle

Fig. 1 Schematic diagram of pintle thruster

The computational model is simplified to 2D-axisymmetric case, for both the pintle and nozzle are axisymmetric and the effect of asymmetric inlet on flow pattern can be ignored. The hot gas consists of reaction products of AP/HTPB/10% Al under the chamber pressure of 8 MPa, which has a total temperature of 3 200 K. In application of SDACS, two thrusters work in a differential working mode to maintain the chamber pressure[5], so the inlet pressure can be treated as a constant value. The ambient pressure is set to be 8 kPa in this paper. All meshes

are structured to ensure good grid quality.

1.2 Dynamic mesh method

Fundamental equations based on the Reynolds-Averaged Navier-Stokes equations are adopted in the mathematical calculation. In Reynolds averaging, the solution variables in the instantaneous (exact) Navier-Stokes equations are decomposed into the mean (ensemble-averaged or time-averaged) and fluctuating components. Substituting expressions of this form for the flow variables into the instantaneous continuity and momentum equations and taking a time (or ensemble) average (and dropping the overbar on the mean velocity, $\bar{u}$) yields the ensemble-averaged momentum equations. They can be written in Cartesian tensor form as:

$$\frac{\partial \rho}{\partial t}+\frac{\partial \rho}{\partial x_i}(\rho u_i)=0$$

$$\frac{\partial}{\partial t}(\rho u_i)+\frac{\partial \rho}{\partial x_j}(\rho u_i u_j)=-\frac{\partial \rho}{\partial x_i}+\frac{\partial \rho}{\partial x_j}(-\rho\overline{u'_i u'_j})+$$

$$\frac{\partial}{\partial x_j}\left[\mu\left(\frac{\partial u_i}{\partial u_j}+\frac{\partial u_j}{\partial x_i}-\frac{2}{3}\delta_{ij}\frac{\partial u_l}{\partial u_l}\right)\right]$$

Due to possible vortex and flow separation in such geometry, the realizable $k-\varepsilon$ turbulence model is used; the wall function method is adopted in the near wall region to improve the calculation accuracy.

In this paper, dynamic mesh method is used to simulate the motion of the pintle tip surface. The moving velocity is given through the user defined function (UDF) to control the movement of the grid.

2 Results and discussion

2.1 Typical flow patterns of pintle thruster

The flow inside thruster presents a complex pattern due to the disturbance of the pintle. Fig. 2 (a) shows the Mach contour and the stream line at 20% opening. The opening is defined as the ration of equivalent throat area and geometry throat area of the thruster. Flowing through the throttle region between the pintle tip and nozzle converging zone, the gas becomes supersonic. Its velocity increases rapidly while pressure and temperature decrease obviously. As a common phenomenon caused by the sudden-expansion geometry, a vortex on the tip of the pintle appears to be tip separation. When the main flow joins with the vortex, there is a lip shock wave generated at the pintle tip, and a compression wave generated on the vortex edge. The two waves combine to be one stronger shockwave after gathering. The combined oblique shock hits with nozzle wall at the expand zone, and is reflected to the axis downstream. Because of the interaction between the shock wave and boundary layer of nozzle wall, the boundary layer becomes thicker at the hit point. What's more, a trailing shock wave is observed near the nozzle axis. Those shock waves make flow become non-isentropic, not only causing losses of total pressure and total temperature but also reducing the nozzle efficiency. Since the opening is very small, the effective nozzle expansion ratio is very large, leading to a 7.4 Mach number at the nozzle outlet.

The hot gas passes through the shock wave so the vortex is a subsonic circumfluence zone indeed, in which the Mach number is below 0.2 and the static pressure and temperature is apparently high. The high pressure on the pintle tip produces an axial aerodynamic force on the pintle. The force is an important influence factor of thruster response speed and cannot be ignored during pintle design[14].

The aerodynamic force is difficult to be measured, for the friction force is coupled in the measured force and hard to separate. As the simulated results show good agreement with experiment results, the force can be estimated by integral of static pressure on the pintle tip surface. A dimensionless coefficient is defined as the following to study the rule of the aerodynamic force:

$$Fp=\frac{\int_{\text{tip}} p\,ds}{F_0}$$

where $F_0=\int_{\text{tip}} p_0\,ds=p_0\cdot S$, p_0 is the inlet pressure, and S represents the sectional area of the pintle tip.

2.2 Effects of thruster opening

Fig. 2 shows the Mach distribution at different

thruster opening. With the opening increasing, the hit point of the combined shock wave moves towards upstream and its angle becomes bigger. Thus the reflection wave deflects towards the axis. When the thruster has a big opening (see Fig. 2 (b)), the reflection waves from upper and lower wall meet at the axis in expand zone, generating another two shock waves towards downstream. The vortex is condensed to have a smaller size with its strength increasing, while the strength of trailing shock wave and the compression wave decrease. What's more, the Mach number of nozzle exit decreases as the effective throat area increases.

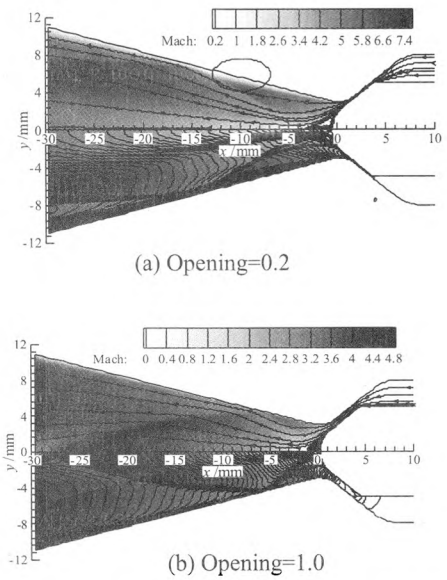

Fig. 2 Mach number contour at various thruster opening

The static pressure distribution on pintle tip wall is presented in Fig. 3. Pressure of various openings shows similar trends. Flowing through the lip shock wave, the pressure has a sudden jump. With the thruster opening increasing, the wave strength increases to produce a higher pressure circumfluence zone. To investigate the effect of inlet pressure on aerodynamic coefficient, flowfields under different conditio (p_c=2~8 MPa) are simulated. The aerodynamic coefficient is a function of thruster opening, but nearly independent of chamber pressure. That is because the distribution law of pressure in different cases is nearly the same for the thruster with fixed surface, which means the ratio of the static pressure and the total pressure are constant at the same position even though chamber pressure is different.

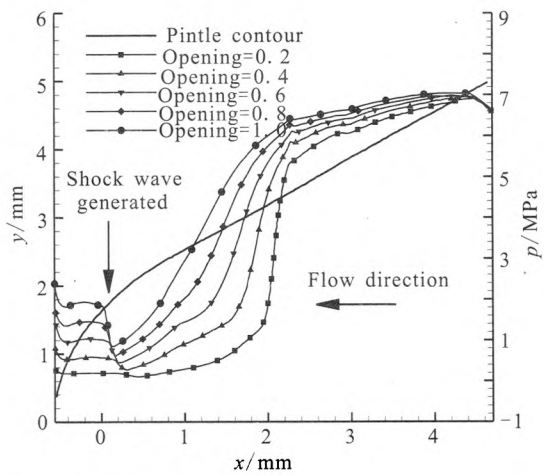

Fig. 3 Static pressure distribution on pintle tip wall of different thruster openings

2.3 Geometrical sensitivity

Tab. 1 Key parameters of calculated cases

Case	α/(°)	r_f /mm	r_p /mm
1	35	7.13	3
2	40	4.24	3
3	45	2.60	3
4	50	1.62	3
5	55	1.01	3
6	40	4.24	0
7	40	4.24	1
8	40	4.24	2
9	40	4.24	4

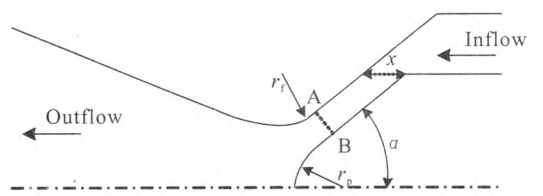

Fig. 4 Schematic diagram of throttling surface

Fig. 4 is the schematic diagram of throttling surface, which is the circular surface formed by AB rotation around the axis. The throttling surface area

is a function of pintle displacement x[15]. The value of key parameters (Tab. 1) is selected based on the principle that the maximum x is kept at a constant value.

2.3.1 Effect of pintle tip radius

Since the static pressure has a rapid decrease when passing through the shock wave, the wave can be presented by calculating the pressure gradient. When the pintle tip radius is zero, the pintle has a cone head indeed. An oblique shock wave is generated at the slope, but no compression wave is observed. That is because the circumfluence zone is nonexistent and the vortex strength is weak. With the radius increasing, the location of the shock wave generating and the hit point move upstream, and a subsonic zone appears with its size becoming bigger, leading to a stronger compression wave.

2.3.2 Effect of throttling surface shape

The shape of throttling surface is controlled by the half cone angle of pintle tip and the throat fillet radius. Static pressure on pintle tip of different shapes is shown in Fig. 5. To make a visualized comparison, the axial coordinate is divided by tip length L to be nondimensionalized. Shape with larger angle and smaller fillet radius tends to have a general higher pressure, leading to a higher aerodynamic coefficient, (see Tab. 2). However, the lip shock waves of different shapes are generated at a nearly same relative position, and wave strengthen has no significant change.

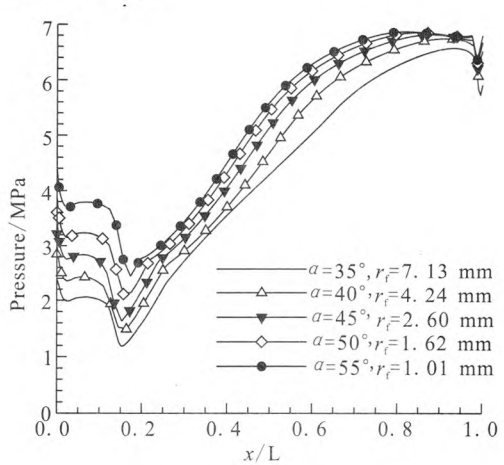

Fig. 5 Pressure distribution on pintle tip with various shapes

Tab. 2 Aerodynamic coefficient of different throttling surface shapes (opening=1.0)

Case	α/(°)	r_f /mm	Fp
1	35	7.13	0.40
2	40	4.24	0.64
3	45	2.60	0.68
4	50	1.62	0.72
5	55	1.01	0.75

3 Conclusions

1) A vortex is observed at the pintle tip which is a subsonic circumfluence zone, leading to high pressure and significant axial force on the pintle.

2) The aerodynamic coefficient varies with thruster opening, but independent of pressure.

3) Pintle tip radius affects the shock wave pattern, and has a positive correlation with subsonic zone size.

4) As the pintle cone angle increases, aerodynamic coefficient increases, while the shock waves are not influenced apparently.

References:

[1] SAYLES D C. The development of test motors for advanced controllable propellants: AIAA 1973-1206[R]. USA: AIAA, 1973.

[2] OSTRANDER M J, BERGMANS J L, THOMAS M E, et al. Pintle motor challenges for tactical missiles: AIAA 2000-3310 [R]. USA: AIAA, 2000.

[3] BURROUGHS S. Status of army pintle technology for controllable thrust propulsion: AIAA 2001-3598 [R]. USA: AIAA, 2001.

[4] MORRIS J W, CALSON R W, PETERSON K L, et al. Multiple pintle nozzle propulsion control system: US 5456425 [P]. 1995-10-10.

[5] ROCK S G, HABCHI S D, MARQUETTE T J. Numerical simulation of controllable propulsion for advanced escape systems: AIAA 1997-2254[R]. USA: AIAA, 1997.

[6] NAPIOR J, GARMY V. Controllable solid propulsion for launch vehicle and spacecraft application[C]// Proceedings of 57th International Astronautical Congress. Valencia, Spain: [s.n.], 2006: 11-18.

(下转第 61 页)

磁成形研究所用的材料本构模型。

4 结论

通过准静态单向拉伸试验和霍普金森拉杆试验建立了考虑应变率的 QCr0.8 铜合金的 Johnson–Cook 本构模型：

$$\sigma=[92+648.4\varepsilon^{0.904}][1+0.0788\ln\dot{\varepsilon}^{*}]$$

该本构模型可用于发动机具有特殊结构的 QCr0.8 铜合金产品及其他行业相同材料产品的电磁成形工艺研究。

参考文献：

[1] 李春峰. 高能率成形技术[M]. 北京: 国防工业出版社, 2001.

[2] 訾炳涛, 巴启先, 崔建忠. 电磁成形设备的国内外概况[J]. 锻压机械, 1998(3): 8-10.

[3] PSY K, RISCH V, KINSEY D, et al. Electromagnetic forming-A review[J]. Journal of materials processing technology, , 2011, 211(5): 787-829.

[4] BALANETHIRAM V S, DAEHN G S. Hyperplasticity-increased forming limits at high workpiece velocity [J]. Scripta metall, 1994 (31): 515-520.

[5] BALANETHIRAM V S, HU X, ALTYNOV M, DAEHN G S. Hyperplasticity: enhanced formability at high rates [J]. Material processing technologies, 1994, 45 (1/4): 595-600.

[6] DAEHN G S, ALTYNOVA M, BALANETHIRAM V S, et al. High velocity metal forming-an old technology addresses new problems[J]. JOM, 1995, 47(7): 42-45.

[7] 李风. 高速率成形中材料本构关系的研究进展[J]. 材料研究与应用, 2008(3): 165-168.

[8] KOLSKY H. An investigation of the mechanical properties of materials at very high rates of loading[J]. Processings of the Physical Society of London, 1949, B62: 676-700.

[9] 韩玉杰. 5A02 铝合金板材磁脉冲成形流动规律研究[D]. 哈尔滨: 哈尔滨工业大学, 2013.

（编辑：陈红霞）

（上接第 24 页）

[7] COON J, YASUHARA W. Solid propulsion approaches for terminal steering: AIAA 1993-2641 [R]. USA: AIAA, 1993.

[8] CAVENY L H, GEILER R L, ELLIS R A, et al. Solid rocket enabling technologies and milestones in the United States[J]. Journal of propulsion and power, 2003; 19(6): 1038-1065.

[9] CAUBET P. Attitude control systems for interceptors[C]// Proceedings of 1st AAAF International Conference on Missile Defense. Arcachon, France: AAAF, 2003: 111-121.

[10] LAFOND A. Numerical simulation of the flowfield inside a hot gas valve: AIAA 1999-1087[R]. USA: AIAA, 1999.

[11] AUSSIGNAC P, UHRIG G.. Theatre BMD: A DACS design for the ASTER Block 2 Kill Vehicle [C]// Proceedings of 4th AAAF International Conference on Missile Defence. Heraklion, Greece, 2007: 22-29.

[12] JONER S, QUINQUIS I. Control of an exoatmospheric Kill Vehicle with a solid propulsion attitude control system: AIAA 2006-6572[R]. USA: AIAA, 2006.

[13] TAO Z J, WANG Y B, LIU Y, et al. Simulation on dynamic response characteristics of electromagnetic gas valve[J]. Computer simulation, 2013, 30(5): 68-71.

[14] CARY L C, ALBERT S D. Rocket thruster comprising load-balanced pintle valve: US8215097[P/OL]. 2010-12-13[2012-07-22]. http://xueshu.baidu.com.

[15] CHANG H, WANG Y B, LIU Y, et al. Experimental investigation of solid attitude control system using proportional pintle thrusters [J]. Applied mechanics and material, 2015, 723(3): 131-135.

（编辑：马　杰）